REACTIVE ASTROGLILOSIS ON ELECTROSPUN NANOSCALE/MICROSCALE FIBER SCAFFOLDS

By

HAN CHEN

A thesis submitted to

the School of Graduate Studies

Rutgers, The State University of New Jersey

In partial fulfillment of the requirements

For the degree of

Master of Science

Graduate Program in Biomedical Engineering

Written under the direction of

David Ira Shreiber

And approved by

_____

_____

_____

_____

New Brunswick, New Jersey

[October 2018]

Abstract of the Thesis

Reactive Astrogliosis on Electrospun Nanoscale/Microscale Fiber Scaffolds

By Han Chen

Thesis Director:

David Ira Shreiber

Astrocytes are glial cells that tiles the mammalian central nervous system. It serves a substantial function in the CNS and the progress of reactive astrogliosis is related to multiple CNS traumatic injuries and diseases. Recent years, the interest in understanding the trigger and the mechanism of reactive astrogliosis has increased and scientists have started to study reactive astrogliosis in vitro on scaffolds like electrospun polymer nanofibers. If it could be understood how various properties of the scaffold can affect reactive astrogliosis, we can then build scaffolds that are able guide/control the process of reactive astrogliosis and implanting such scaffolds in diseased brain tissue would become new treatment methods. In this project/thesis, effects of the orientation of electrospun nanofibers and the nanofibers of different materials on reactive astrogliosis have been studied. Results found that the orientation of the fiber scaffold can affect the extent of reactive astrogliosis and fiber diameter is a dominant factor than the chemical properties of the polymer. However, further study analyzing the effects other chemical and physical properties of the polymer scaffold on reactive astrogliosis needs to be done to fully understand the role of polymer nanoscale/microscale fiber scaffold in reactive astrogliosis.

Acknowledgement

I would like to acknowledge the individuals who have provided extraordinary assistance and support in this project. I am grateful for my personal instructor, David Ira Shreiber, Ph.D., for giving me care and guidance in my life and graduate career. I am also grateful for David Sillitti, who was the previous master's student in the reactive astrogliosis and electrospinning project, for mentoring me when I joined the lab and this research program. I would like to thank Ahmed Ijaz, our lab research assistant, for helping me in setting up primary cell culture. I am appreciative of Xin Liu, a Ph.D. candidate in the Program of Biomedical Engineering, for assisting me in using Scan Electron Microscopy. I am also thankful for other previous and existing graduate students in the Shreiber Lab, Chris Lowe, Madison Godesky, Yoliem Miranda Alarcon, for helping me in working in the lab. Lastly, I would like to thank my parents and grandparents for their lasting love and support.

Table of contents

List of figures

List of tables

Chapter 1. Introduction

1.1 Astrocyte morphology, physiology, and reactive astrogliosis

Astrocytes are specialized star-shaped glial cells that exist in the central nervous system (CNS) and serve multiple structural and functional roles in CNS.

There are two types of astrocytes categorized by their morphology and anatomical locations. One is called protoplasmic astrocyte; it exists in the gray matter and has a morphology of many fine branched processes reaching outward from five to ten stem branches. [1] Protoplasmic astrocytes can envelop synapses, and monitor and alter synaptic function. [1-3] The other one is called fibrous astrocyte: this type of astrocyte is found throughout white matter and has a morphology of many fiber- like long processes reaching out from the cell body. [1] These processes of fibrous astrocytes connect to nodes of Ranvier. Both types were found to be extensively contacting blood vessels, controlling blood flow and forming gap junctions between neighboring astrocytes. [1] In healthy CNS, astrocytes tile the entire CNS without overlapping. Only the tips at the very end of the processes of individual astrocytes contact with each other.

Figure 1: Protoplasmic astrocyte and fibrous astrocyte

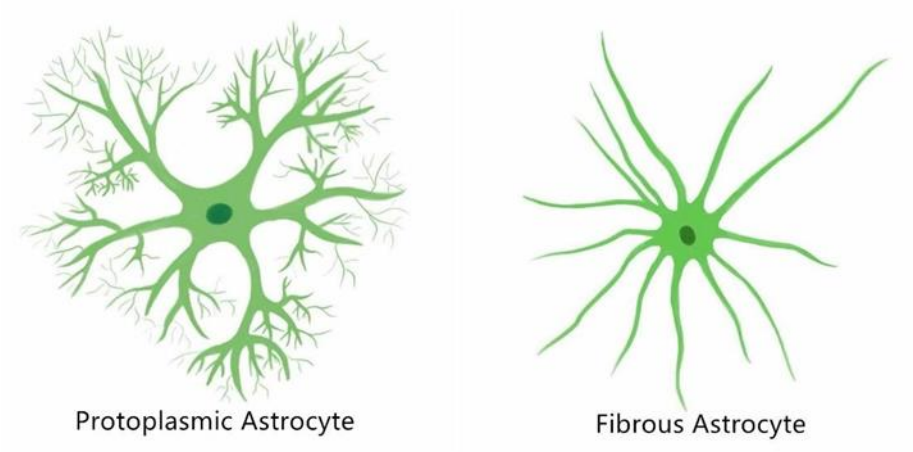

There are different molecular markers for astrocytes. One widely used marker is glial fibrillary acid protein (GFAP). GFAP is an intermediated filament protein expressed by many types of cells in the central nervous system. [4-6] It was first isolated from multiple sclerosis patients' demyelinated plaques and reactive astrocytes was found to be associated with it in such plaques and in other pathological contexts. [1, 4-5, 7] However, double staining with multiple markers showed that some healthy astrocytes often do not express detectable level of GFAP and the expression of GFAP by astrocytes has regional differences. Also, it is found in transgenic mice that GFAP expression is not essential for the appearance and function of most astrocytes in healthy tissues but is essential for reactive astrogliosis and glial scar formation. [1] According to these findings, GFAP expression can be considered as a reliable marker for most reactive astrocytes, or say, reactive astrogliosis, in CNS injuries.

Reactive astrogliosis is a process of astrocytes responding to all kinds of CNS injuries and many intracellular molecules can trigger. It is a finely gradated continuum of progressive

changes of astrocytes in gene expression and cellular changes. [1] In the process of reactive astrogliosis, changes in astrocyte morphologies and functions occur. [8] The extent of reactive astrogliosis can be graded from mild to severe.

In mild to moderate reactive astrogliosis, GFAP expression increases with cell body enlargement and cell process growth, while individual cell domains remain. [1, 8] Mild non-penetrating and non-contusive trauma are usually related with mild to moderate reactive astrogliosis. [1] This stage of astrocyte astrogliosis is potentially reversible if astrocytes can regain an appearance similar to healthy ones. [1, 9] The next stage is severe diffuse reactive astrogliosis. In this stage GFAP expression and cell body and process growth are all pronounced. The extension of the cell processes could intermingle and overlap with the neighboring astrocytes, leading to the loss of individual cell domains. [1, 9] This stage of reactive astrogliosis can be found at sites around severe focal lesions and chronic neurodegenerations. [1] A more advanced stage is severe reactive astrogliosis. This stage engages pronounce upregulation of GFAP expression, pronounced cell body hypertrophy, and pronounced process growth, and usually includes compact glial scar formation. Additionally, because of the pronounced cell process growth, the individual domains of cells are eradicated while dense, narrow, compacted glial scars are formed at the intersection of the reactive astrocytes, fibromeningeal, and other glial cells. [1, 8] Severe reactive astrogliosis is associated with long-lasting and non- reversible tissue reorganization and structural change. This stage of reactive astrogliosis can be found in severe trauma, invasive infections, and chronic neurodegeneration. [1]

Figure 2: Stages of reactive astrogliosis

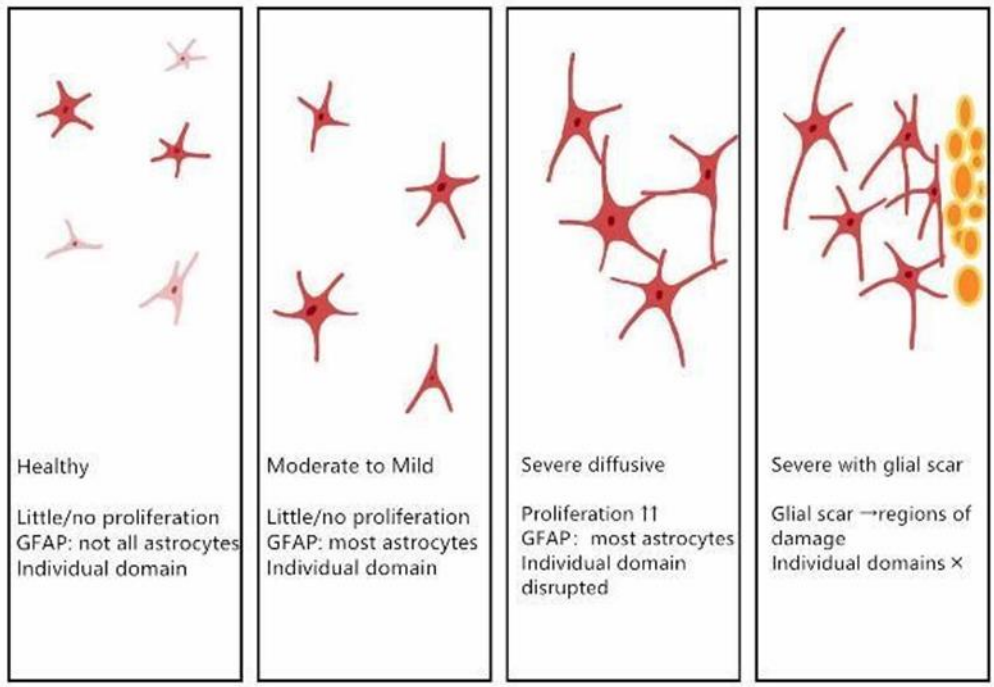

There are many different triggers for reactive astrogliosis. These triggers include large polypeptide growth factors and cytokines, mediators of innate immunity, neurotransmitters, reactive oxygen species, hypoxia and glucose deprivation, neurodegeneration products, regulators of cell proliferation, molecules related with systemic metabolic toxicity, etc. [1] Different stimuli trigger different signaling mechanisms in reactive astrogliosis. For example, intracellular signaling pathway related with cyclic adenosine monophosphate (cAMP), the derivative of adenosine triphosphate (ATP), is found to mediate GFAP upregulation, while epidermal growth factor (EGF) can lead to reactive astrocyte proliferation. [1]

In the past, it was thought that reactive astrogliosis is a maladaptive process that leads to inflammation and pain so that inhibiting reactive astrogliosis was a therapeutic goal.

However, with the advance of study and research, reactive astrogliosis is found to have beneficial effects that protects CNS by 1) uptake of excessive glutamate that might be excitotoxic; 2) degradation of amyloid-beta peptides; 3) facilitation of blood-brain-barrier repair, 4) prevention of inflammatory cells and infectious agents spreading from diseased tissue to healthy tissue, etc. [1] Hence, reactive astrogliosis could be understood as a model that exerts different functions under various scenarios: it could be pro-inflammatory at the early stage of insult, but also can be anti-inflammatory when there is intense inflammation. [1, 10]

The goal of treating CNS injuries that relate to reactive astrogliosis requires our ability to understand and control the behavior of astrocytes, which then gives rise to the need of mimicking natural ECM in vitro so that we can seed astrocytes and study reactive astrogliosis on that scaffold. Electrospun polymer fibers could be a choice since it can represent the matrix like structure of the ECM.

1.2 Electrospinning

Electrospinning is a method that has been practiced in recent years to fabricate fibers nanoscale or microscale in the engineering field. The history of electrospinning could be dated back to more than a hundred years ago. The phenomenon was first observed by Lord Rayleigh in 1897 and was patented by Formhals Anton in 1934. [11] Since then, people have been studying and improving this technique using multiple polymer melts and solutions. It is found that till 2013 there are more than 1891 electrospinning patents. [12] The use of electrospinning has been applied to many different biomedical areas including

tissue engineering, wound dressing, drug delivery, et cetera. [11]

Figure 3: Applications of electrospun fibers in biomedical engineering

The process of electrospinning utilizes electrostatic forces to pull out prepared polymer solution from the thin end/tip of the loaded spinneret, and then forms fibers on the collecting surface while the solvent in the solution evaporates and the polymer turns back into solid. There are two standard electrospinning setups, horizontal and vertical. In the vertical setup, a spinneret is loaded above the collecting surface while the tip of the spinneret is connected to a high voltage positive electrode and the collecting surface/collector connected to a negative electrode. Similarly, in the horizontal setup, the spinneret is positioned horizontally with the tip pointing towards the collecting surface with the same electrode setup. The electrospinning equipment is usually set up in a vented chamber in order to avoid the unpleasant smell of the solvent/polymer and inhalation of some toxic/carcinogenic solvent.

Figure 4: Electrospinning setups

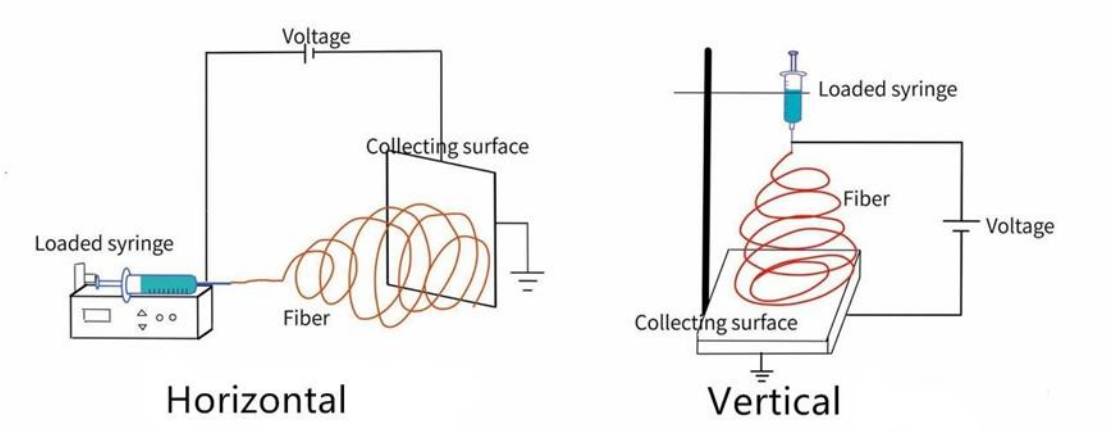

Multiple polymers have been used in electrospinning and then applied to varying fields. These polymers can be categorized into natural polymers, synthetic polymers and copolymers. [11] Common used polymers include silk fibroin, collagen, chitosan, polyglycolide (PGA), poly-L-lactide (PLLA), polycaprolactone (PCL), polystyrene (PS), et cetera. The application of these polymer fiber scaffolds varies due to their different chemical and physical properties.

1.3 Importance of the study

The morphology of astrocytes is strongly related to CNS disorders including CNS trauma, stroke and cerebrovascular disease, infection, seizure disorders/epilepsy, multiple sclerosis, blood-brain-barrier integrity, hepatic encephalopathy, metabolic disorders, Alzheimer's disease, Parkinson's disease, Amyotrophic lateral sclerosis (ALS), tauopathies, Huntington's disease, brain tumors, et cetera. and is a useful indicator in studying reactive astrogliosis in vitro. [1, 13-18] It is necessary we understand the mechanism and trigger of reactive astrogliosis so that we can create new therapeutic strategies to involve astrocyte

activities in the treatment process.

The electrospun nano/microscale fibers scaffolds are far away from mimicing the natural ECM but to some extent, it is a step forward. By changing different properties of the scaffold and seeding astrocytes on these scaffolds, we get the chance to analyze the effect of each single property on the morphological change in reactive astrogliosis. Since there are too many variables in the electrospun fiber scaffold, only a few of them were analyzed in this research. Indicators of the reactive astrogliosis including the number of cells, process length, cell area were analyzed and discussed.

In the rest part of this paper, we will talk about reactive astrogliosis on random vs. aligned fibers first, following by reactive astrogliosis on scaffolds of the same size but different materials, and end with discussion of the study and conclusion.

Chapter 2. Reactive Astrogliosis on Random Fibers vs. Aligned Fibers

2.1 Introduction

One goal of overcoming the glial scar is to enable axons to regenerate around/through an injury site following SCI. [19,20] One idea is that aligned astrocytes may encourage aligned axon growth. [21,22] In previous work that was done in our lab, we have cultured astrocytes on random PLLA fibers and found that astrocyte processes tend to follow the fibers and have increased length as the diameter of electrospun poly-L-lactic acid (PLLA, synonym poly-L-lactide) nanofibers increase. While doing literature search, we found that scientists in Singapore have used random and aligned PLLA nanofibers to culture neural stem cells. It is found that the neuron stem cells (NSCs) elongated on the aligned scaffolds and neurite outgrowth were oriented along with the fiber direction, whereas the fiber diameter did not show any significant effect on the cell orientation. [23] This then raised us the curiosity and decided to test if the aligned fiber scaffold have any influence the orientation of astrocytes.

The goals for this part of the experiment are: 1) obtain random and aligned fibers using electrospinning, 2) seed quiescent and reactive astrocytes on these fiber scaffolds, and 3)analyze the influence of fiber distribution on reactive astrogliosis.

2.2 Materials and methods

2.2.1 Selection of Material: Poly-L-Lactide

Polylactide is a thermoplastic aliphatic polyester that has a long history of safe use in

medical applications such as pins, plates, screws, intra-bone and soft tissue implants. [24] Poly-L-lactide acid is the product of polymerized L-lactide, it turns into glass transition state at 60-65 degrees Celsius, melts at 173-178 degrees Celsius and has a tensile modulus of 2.7-16MPa. PLLA is biodegradable, biocompatible, and biologically inert. It is a polymer that can degrade over months in physiological conditions.

PLLA has been used in the biomedical field in various forms: US Food and Drug Administration (FDA) proved PLLA-based injectable medical device for restoration and correction of HIV-associated facial fat loss in 2004, PLLA/hydroxyapatite scaffolds were tested in vitro for bone tissue engineering, PLLA membranes were proved to be genotoxicological safe and can be used in drug delivery systems. [24-26] The properties and scientific findings/applications made that PLLA a suitable material in testing reactive astrogliosis.

Also, in previous trials that were done in our lab on electrospinning PLLA, we found that PLLA is easy to tailor, complies to changes in electrospinning, and can form fibers in a wide range (200nm to 1100nm). This gives us the confidence to electrospin aligned PLLA fibers.

2.2.2 Culture Surfaces preparation

Nanofibrillar scaffolds were prepared using the method of electrospinning. 12mm circle cover slides (Carolina) are fixed on aluminum foil using lab tape. The aluminum foil with the slips is then wrapped on the mandrel of the electrospinning machine. Poly-L- lactide (PLLA) is weighed to the desired amount and then dissolved in dichloromethane (DCM)

and dimethyl formamide (DMF). The ratio of DCM to DMF is 4:1 (DCM: DMF). Usually, DCM was added first to fully dissolve with the polymer overnight or an even longer time, depends on the concentration of the desired final solution. DMF was then added later and mixed using a magnetic bar on a stirrer for around 1~2 hours until the solution is uniform. Then the solution is loaded into a 5mL syringe with an 18- G needle. The syringe is secured to the syringe pump and is ready for electrospinning. The setup for electrospinning random PLLA nanofibers is 6000RPM for the mandrel, 5ml/hr for the syringe pump's flow rate, 15kV for the applied voltage and the distance between the needle and the mandrel is 7cm. After desired amount of fibers were collected, the aluminum foil was removed from the mandrel. The fibers were then fixed to the edge of the coverslips using Silicon Adhesive (FACTOR II INC) before taking the coverslips off from the aluminum foil, this step prevents the detaching of the fibers in the cell culture process.

The method to obtain aligned fibers by electrospinning is to increase the speed of the mandrel. By increasing the speed of the rotating mandrel, the tensile force applied on these fibers increase. When there is enough tensile force, fibers get stretched and stick to the collecting surface in an aligned way.

Confirmation of the alignment of the fibers was done with Olympus Scope IX81 (Life Science Solutions). In Figure 5, which was taken in the bright field, most fibers are oriented in a vertical direction with a small part of fibers randomly distributed, proving that the desired alignment of the fibers was achieved.

Figure 5: Electrospun aligned PLLA fibers

A higher degree of alignment could be achieved by increasing the rotation speed of the mandrel. However, our electrospinning equipment became unstable and experiences a violent vibration when the speed of mandrel increased above that used to generate Figure 5.

Random and aligned fibers made from 11% 13% and 15% PLLA solutions were prepared for the experiment.

2.2.3 Primary astrocyte acquirement and culture

Primary quiescent astrocyte and primary reactive astrocyte cell culture were prepared as follows. Neonate rat pups were decapitated and their brains were isolated aseptically. Hemispheres were separated and cerebral cortices were dissected out. Meninges were removed to avoid fibroblasts in the cell culture. These steps were done in dissection media. After obtaining the cerebral cortices, they were cut into small pieces and digested in 0.1%

trypsin and 0.02% DNase at 37°C for 20 minutes to be softened. The softened tissues were pipetted through a fine pipette tip up and down several times to obtain a cell suspension. The cell suspension was then filtered with a 40um mesh, large clusters of cells were removed in this step, and a single cell suspension could be obtained. For cell culture, the single cell suspension was placed in T75 flasks (one brain per flask) and incubated in water jacked CO2 incubators at 37°C. Culture medium was changed every 3 days to remove cell debris until the cells reached confluency. The cultures usually reach confluency in 7 days, and then quiescent astrocytes are ready to use. To get reactive astrocytes, the amount of fetal bovine serum in culture medium was reduced to 1%, and 0.25mM dbcAMP was added. Astrocytes cultured with dbcAMP were usually incubated for 7-8 days. All animal use procedures were viewed and approved by the Rutgers Animal Care and Use Committee and included in Protocol #02-004.

2.2.4 Seeding, immunostaining, and imaging

The scaffolds were seeded with quiescent or dbcAMP-treated astrocytes for 24 and 48 hours with the number of 30000 cells/well. After the culture, the medium was removed, and then 4% paraformaldehyde was added to fix the cells for 10 minutes. The paraformaldehyde retains the quaternary protein structure for later Phalloidin staining. The paraformaldehyde was then removed, and the slides were rinsed with PBS 3 times. Then 0.5% Triton X-100 in PBS was added to permeabilize the cell membranes. After 5 minutes, Triton X-100 was removed and the cells were blocked with 10% normal goat serum for 30 minutes. The use of normal goat serum is for reducing non-specific binding of proteins and

antibodies to reaction surfaces and non-specific binding sites. Then normal goat serum was also removed, and the slides were rinsed with PBS 3 times. Cells are triple stained for Glial Fibrillary Protein (GFAP), F-actin and the nucleus.

Rabbit anti-GFAP is the primary antibody. Cells were incubated in a 1:500 dilution of the antibody overnight at room temperature. The primary antibody was then removed and the slides were rinsed three times with PBS. The secondary antibody is goat anti- rabbit Alexa 568 IgG, it was diluted 1:500 and incubated with the cells at room temperature for 1 hour. Then the secondary antibody was also removed and the slides were rinsed again 3 times with PBS. Phalloidin 488 is used to stain the F-actin. It was diluted 1:100 and then incubated with the cells at room temperature for 1 hour. Remove the Phalloidin and rinse again with PBS 3 times. Finally, the slides were mounted and stained for DAPI using Fluoro-Gel II Mounting Medium with DAPI on microscope slides. The samples were then ready for imaging on the Olympus Scope IX81.

2.3 Result

2.3.1 Descriptive analysis

Figure 6: Quiescent astrocytes cultured for 24hr

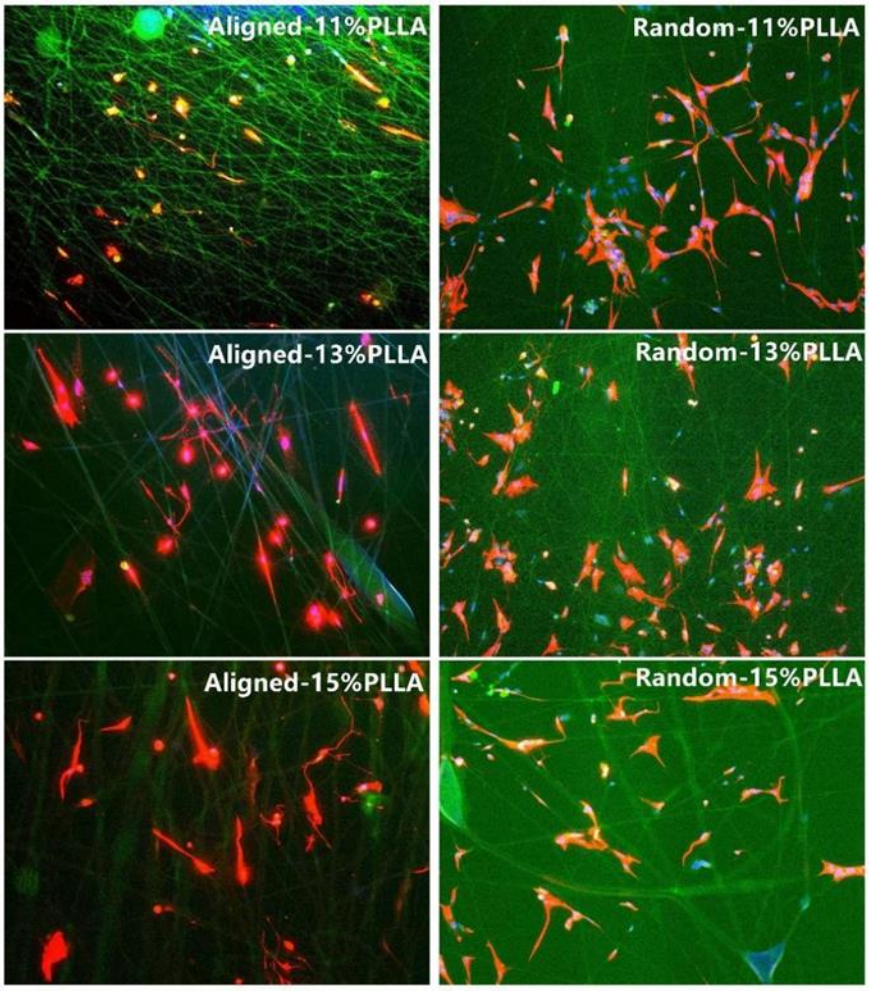

Figure 7: dbcAMP treated astrocytes cultured for 24hr

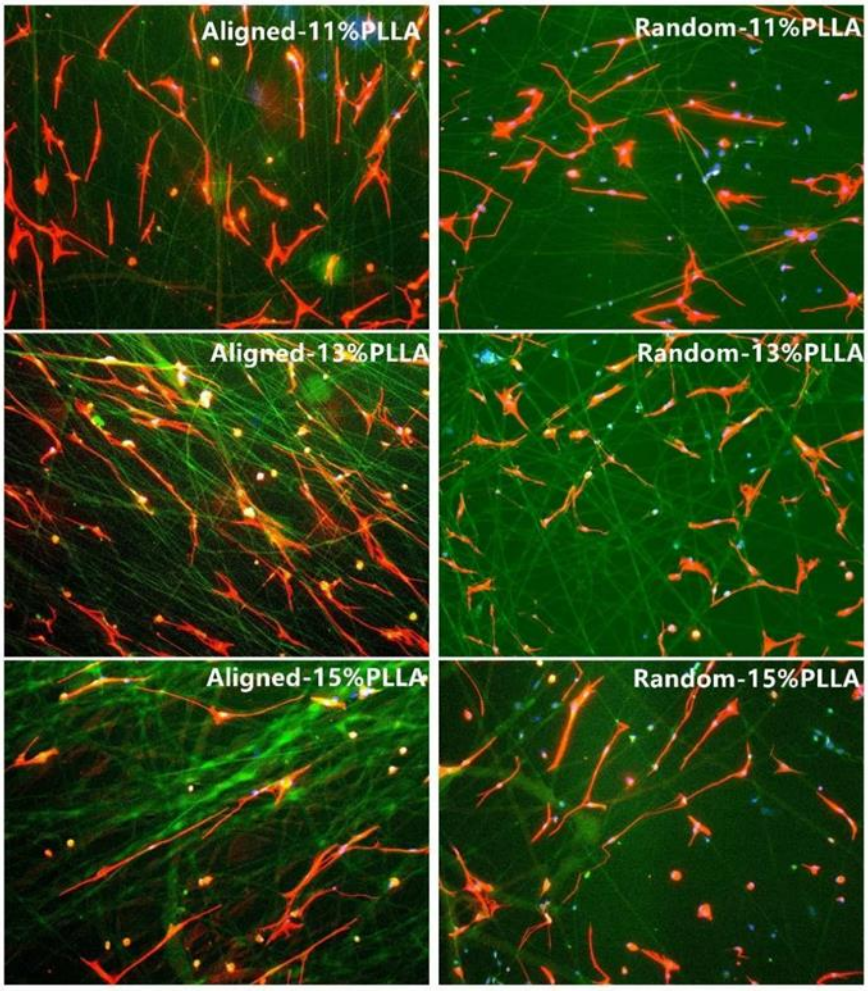

Figure 8: Quiescent astrocytes cultured for 48hr

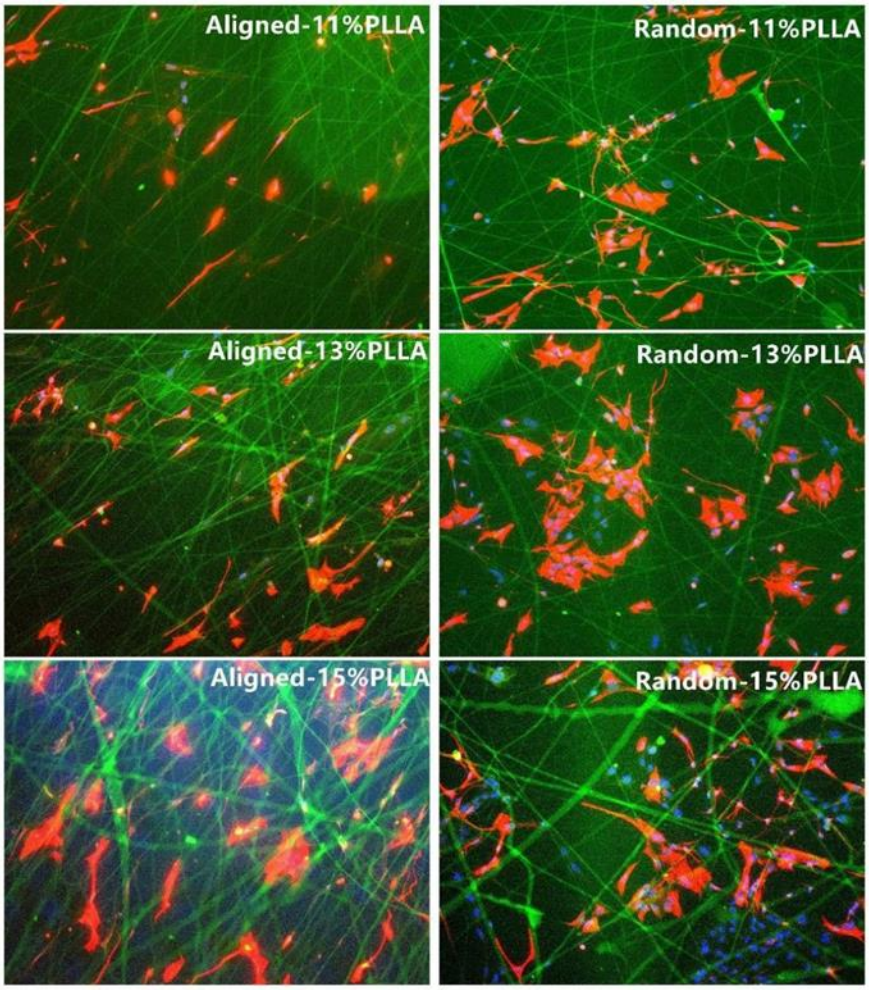

Figure 9: dbcAMP treated astrocytes cultured for 48hr

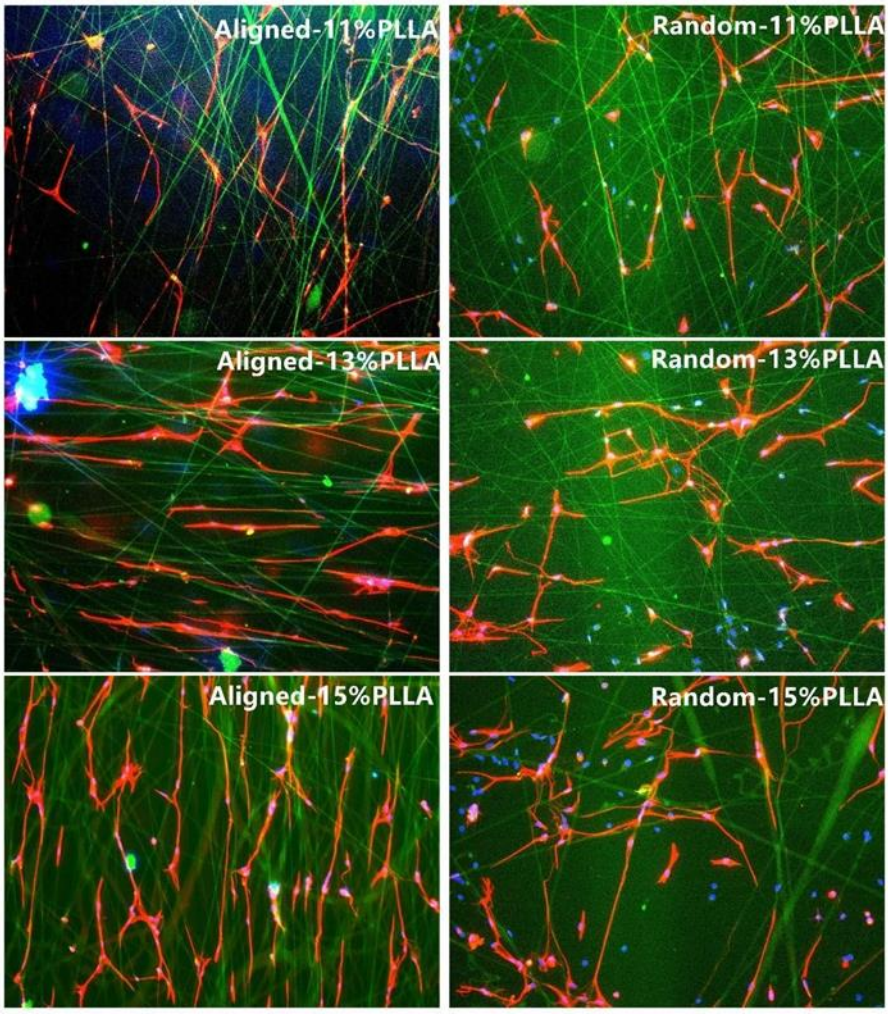

The images selected here are representative of each scenario. It can be seen from the images that: 1) quiescent astrocytes generally have less and shorter process than the reactive astrocytes, some of them are still circular, 2) reactive astrocytes have longer and thinner processes and their shape are elongated, 3) astrocytes growing on aligned fibers showed a polarity that they tend to reach out the process in the direction of the fibers.

2.3.2 Quantitative analysis

a) Proliferation

The average number of astrocytes per image was measured and compared to tell the proliferation difference in reactive astrogliosis on aligned and random fibers.

Figure 10: Number of astrocytes on aligned fibers

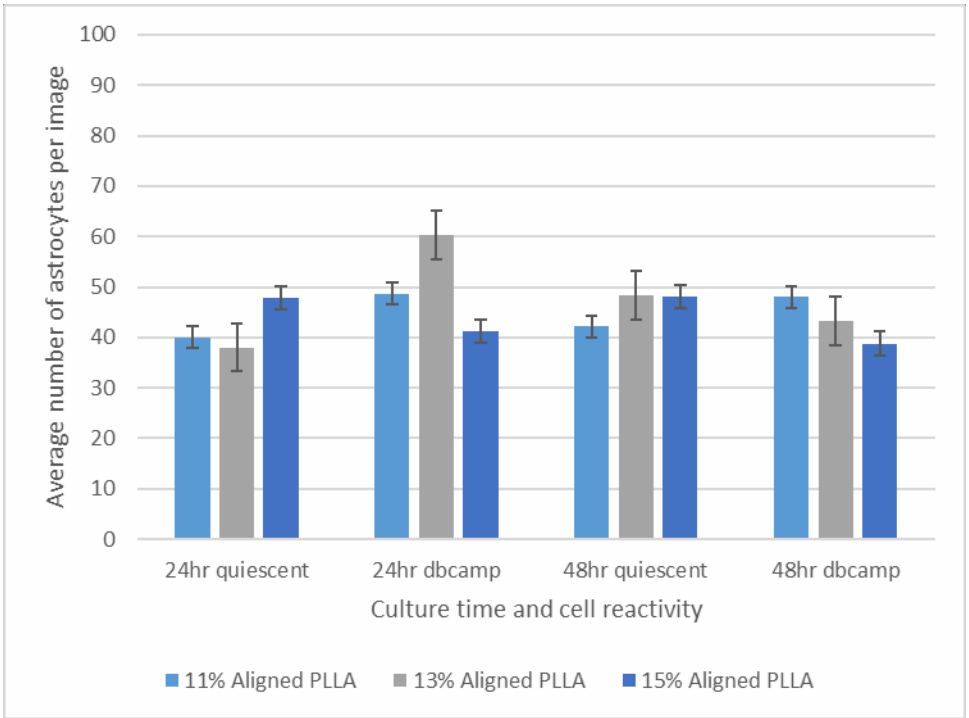

Figure 11: Number of astrocytes on random fibers

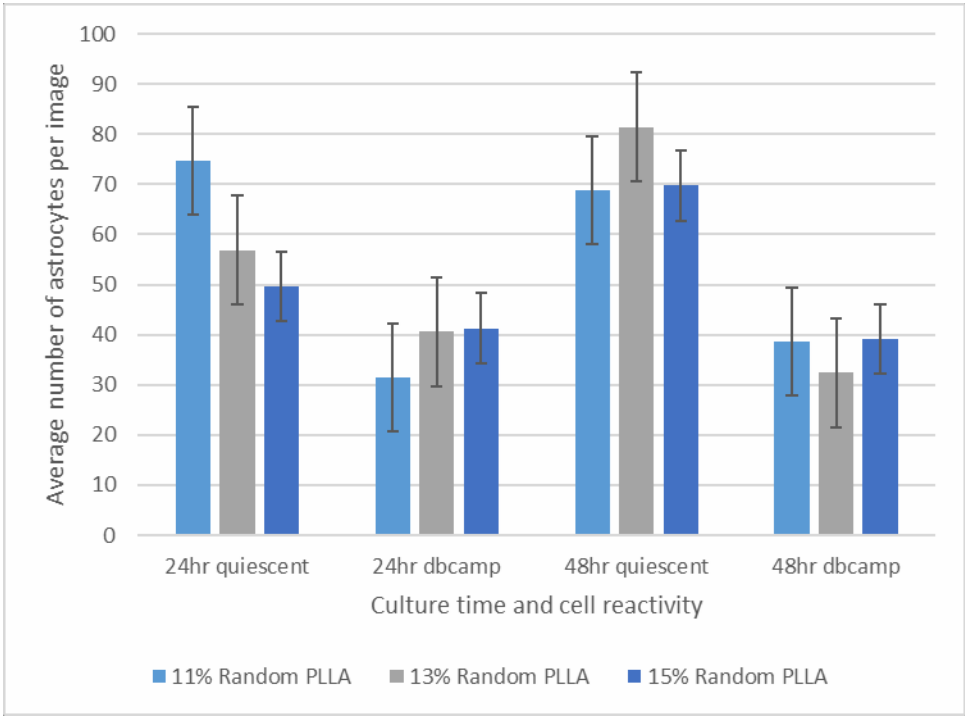

In the aligned fiber group, there seems to be no trend. One-way ANOVA's (with a significant factor of 0.05) results on fiber diameter, culture time, and cell type was also done. The P-values of 0.73, 0.74 and 0.48 showed that there is no significant difference in cell proliferation in these different categories. While in the random fiber group, it can be seen that: 1) scaffolds seeded with quiescent cells have more cells than scaffolds seeded with dbcAMP treated cells, 2) scaffolds seeded with quiescent cells have a decrease in cell count while the fiber diameter increase, 3) scaffolds seeded with dbcAMP treated cells have an increase in cell count while the fiber diameter increase. The results were again analyzed with ANOVA. P-value results of 0.96, 0.58 and 0.0001 proved that there is no difference in the cell count according to fiber diameter or culture time but a difference in seeded cell type.

The difference between the aligned group and the random group was not expected. However, since the two groups were not done at the same time and seeded with the same batch of cells, it is possible that the difference is due to different batch of cells.

b) Process length

Process length is also an indicator of reactive astrogliosis. It is proposed that astrocytes growing on aligned fibers will have longer processes due to fewer distractions of random fibers.

Length of processes was measured by ImageJ and the averages were calculated, results are plotted as below.

Figure 12: Astrocyte process length on random fibers

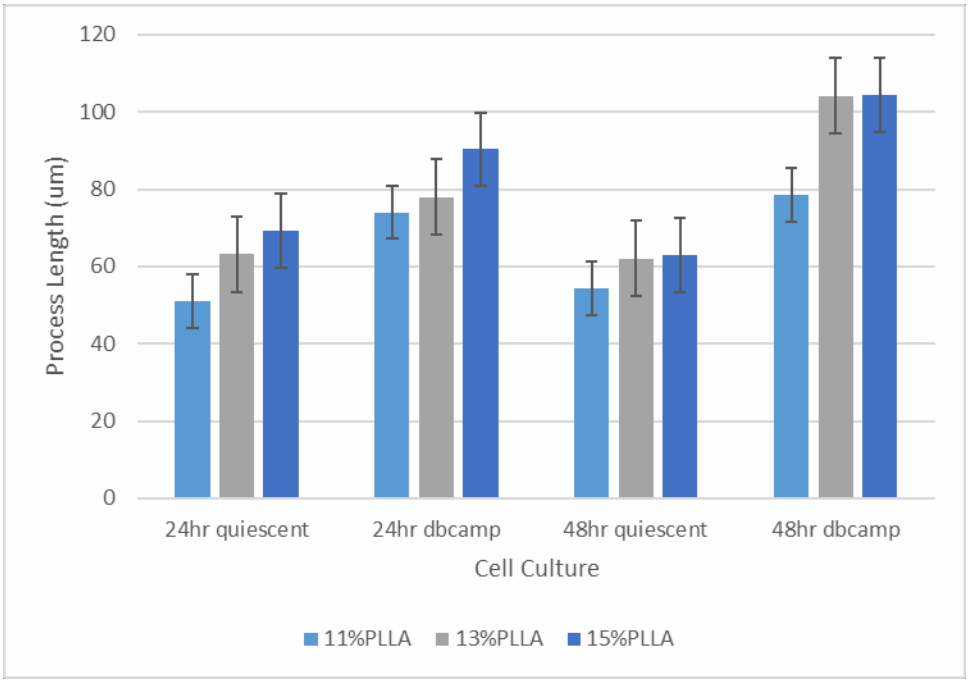

Figure 13: Astrocyte process length on aligned fibers

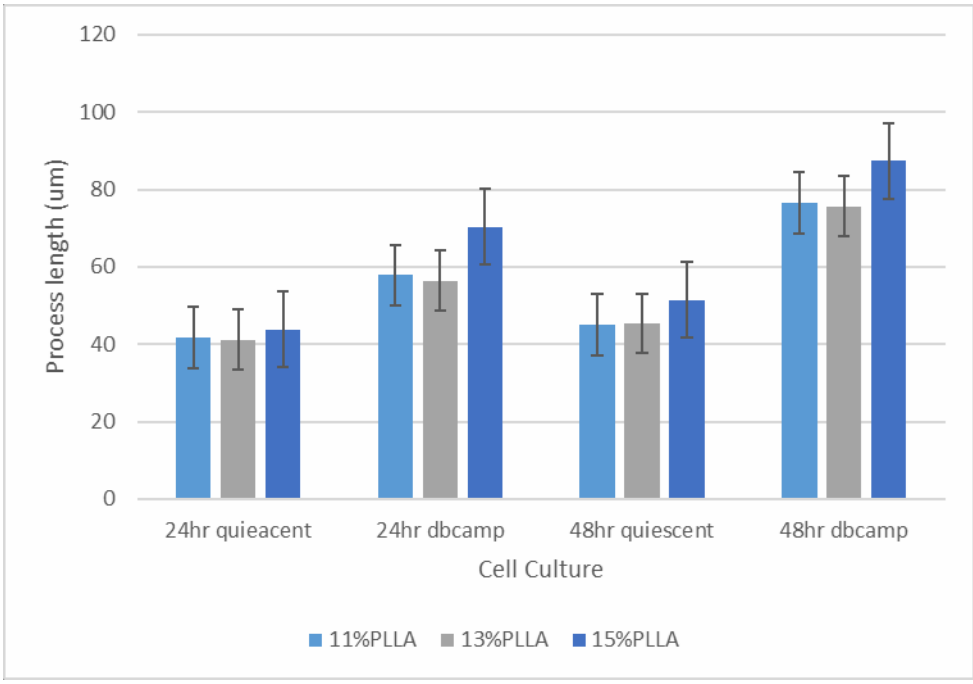

In the random fiber group, 1) cells cultured for 48 hours have longer processes than cells cultured for 24 hours, 2) dbcAMP treated cells have longer processes than quiescent cells, 3) after 48 hours, dbcAMP treated cells have a longer growth in processes than quiescent cells.

In the aligned fiber group, 1) quiescent cells have a decreased length in processes after 48 hours than after 24 hours, 2) dbcAMP treated cells have increased length in processes as culture time increase, 3) dbcAMP treated cells have longer processes than quiescent cells. ANOVA test between random fibers and aligned fibers came out with a P-value of 0.024 which is smaller than α of 0.05, and two averages of 57.73 and 74.35. The results demonstrated that astrocytes on the aligned PLLA fibers generally grow longer than on the random PLLA fibers. This corresponds with our expectation that the many intersections of

the fibers in the random fiber scenario distracted and suppressed the growth of the processes.

c) Process alignment with fibers

If we want to know if the how are astrocytes oriented by the fibers in aligned fiber scenario, it is necessary to analyze the angle between each single cell process and the closest fiber. This was analyzed with ImageJ's "Angle" tool and the distributions in angle were plotted as box and whisker plots.

Figure 14: Alignment of quiescent astrocytes' processes on aligned fibers

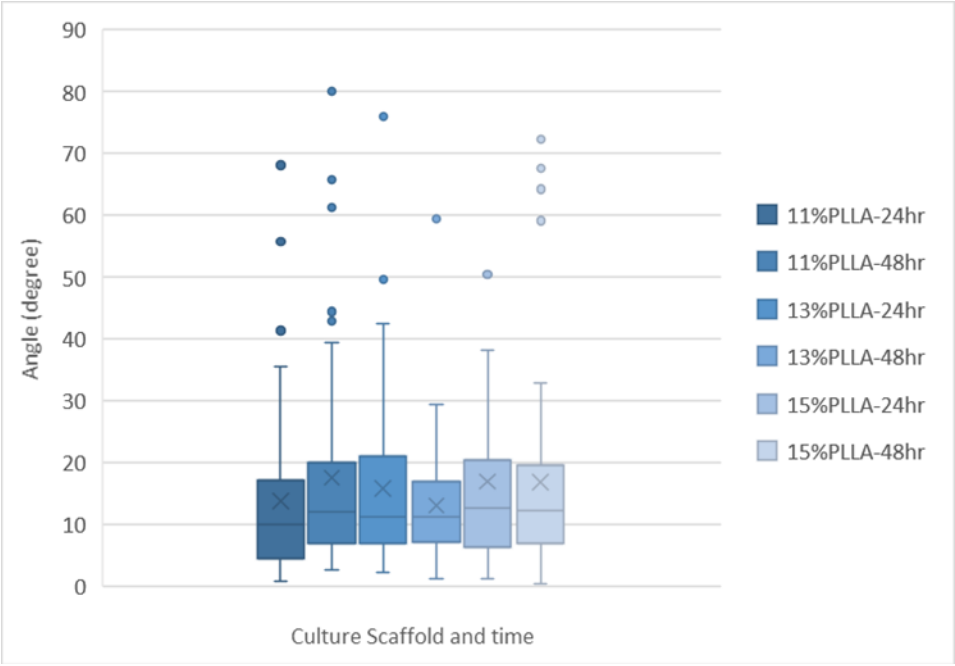

Figure 15: Alignment of dbcAMP treated astrocytes' processes on aligned fibers

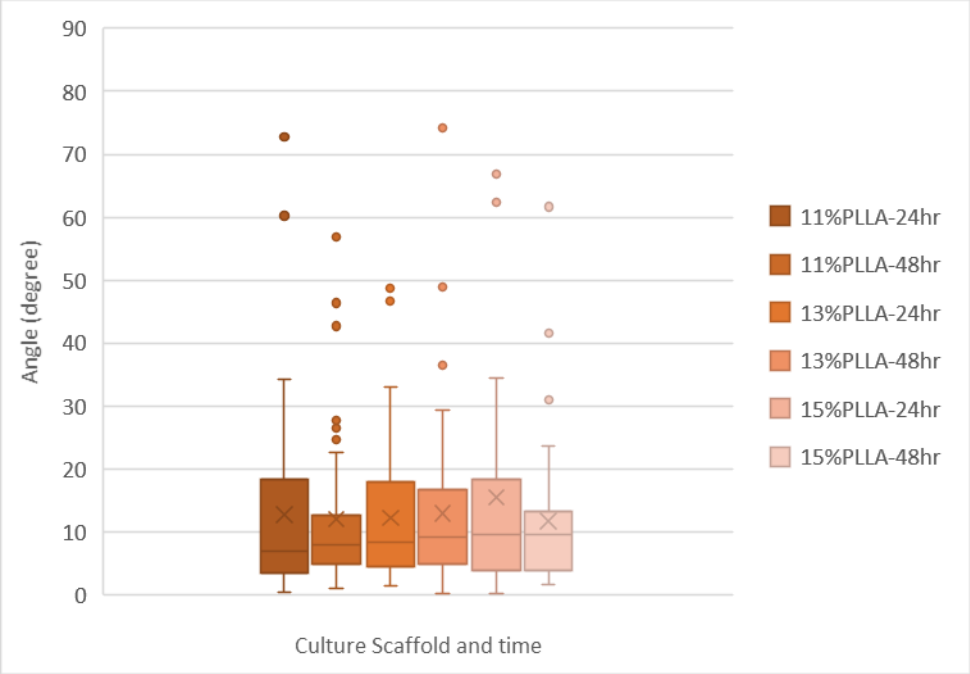

Figure 16: Alignment of quiescent astrocytes' processes on random fibers

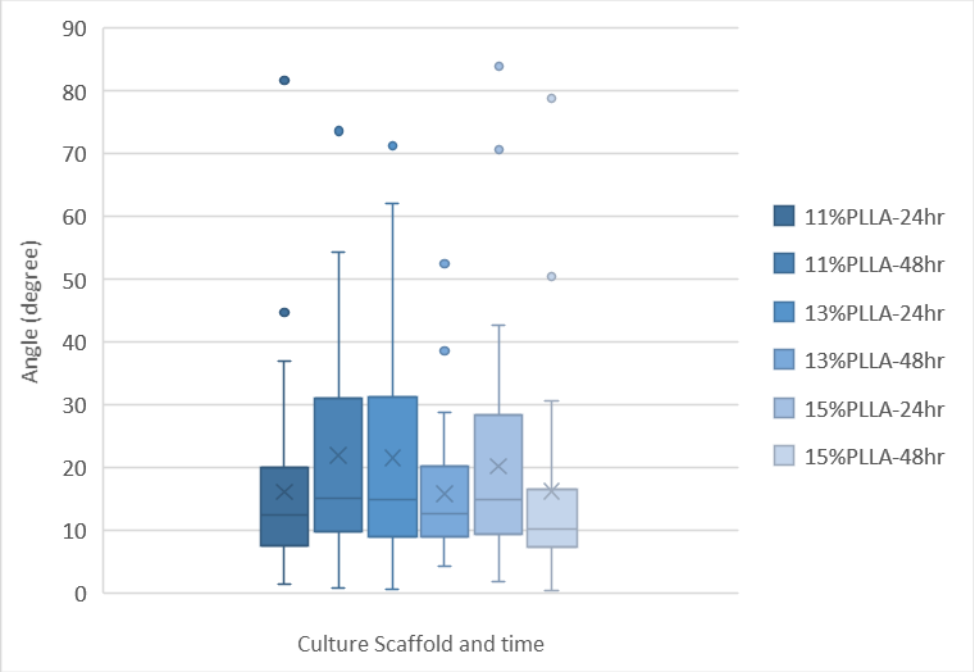

Figure 17: Alignment of dbcAMP treated astrocytes' processes on random fibers

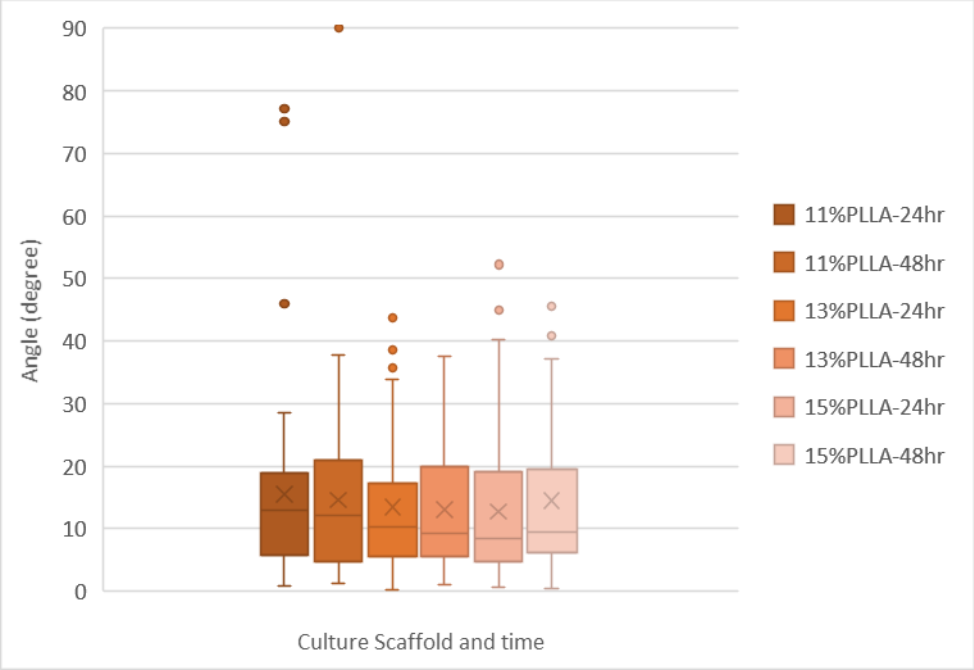

If we apply the same criteria as Yang, Murugan, Wang and Ramakrishna [23], define that the angle between 0 and 10 degrees represents processes are aligned with the fibers and angle between 80 and 90 degrees represents processes are perpendicular to the fibers, then according to the distribution in the plots, more processes tend to follow the fibers in the aligned fiber scenario.

One-way ANOVA tests were also done in to test the influence of other variables: seeded cell reactivity, culture time, fiber diameter and fiber alignment. The P-values are 0.009, 0.82, 0.47 and 0.037. The results showed that: 1) the mean angle in quiescent and dbcAMP treated astrocytes are significantly different, dbcAMP treated astrocytes tend to have smaller angles between processes and fibers, 2) there is no significant difference in astrocyte processes alignment to fibers with different culture time, 3) there is no significant

difference in astrocyte process alignment with different fiber diameter and that fiber diameter does not have an influence on the orientation of astrocyte processes, 3)there is significant difference in astrocyte process alignment in fiber orientation, the angles are smaller on aligned fibers.

d) Process number

The number of processes per cells is also counted and the modes are compared. It is found that most astrocytes seeded on aligned fibers have only 2 processes, some have 3 processes, and a few have multiple processes more than 3. While in the random fiber group, more astrocytes have more than 2 processes. Another feature that can be observed in the aligned fiber group is that in an astrocyte that has multiple processes, the processes that are not following the fibers are much shorter than processes following the fibers.

2.4 Conclusion

In this chapter, the formation of random and aligned PLLA fibers using electrospinning and analysis of reactive astrogliosis on these fiber scaffolds were discussed. Indicators including the number of astrocytes, the number of processes per cell, average process length and angle between processes and fibers were measured. Results showed that compared to random fibers, aligned fibers can promote the growth of process length but induce less amount of processes per cell.

Chapter 3. Reactive Astrogliosis on PLLA and PCL Nano/Micro Fibers

3.1 Introduction

The results of our previous study that the increase of PLLA nano/micro fiber's diameter can promote reactive astrogliosis also give rise to another question: is this dependent on size for PLLA only or does it also hold for other polymers? To examine our question, in this chapter, we will talk about electrospinning another polymer and compare its impact on reactive astrogliosis with PLLA.

Random nanofibers made from PLLA and another polymer that are of the same diameter range are desired for the experiment. By doing so, we would be able to have a control on one variable and analyze whether fiber diameter or other properties of the polymer material has/have more effect on reactive astrogliosis. To achieve this, we must first identify the conditions to generate fibers of the same size then repeat the culture experiments.

3.2 Materials and Methods

3.2.1 Selection of material

Polycaprolactone (PCL) is a polyester with a glass transition temperature of -60 degrees Celsius and a melting temperature at around 63 degrees Celsius. Because of its high crystallinity (usually 50%) and hydrophobic nature, the degradation of PCL is relatively slower than PLLA. [27] PCL has also been applied in many fields in biomedical engineering like long-term implants and controlled drug release. [28] There is also lots of research done with electrospun PCL nanofibers: electrospun heparin-bonded PCL fibers

were proved to be a suitable graft for small artery reconstruction, electrospun PCL coated with chitosan-silver nanoparticles were found to have increased biocompatibility, mechanical strength and antibacterial activity against both Gram- negative and Gram-positive bacteria and hence were promising in wound dressing. [29,30]

The properties and these research findings suggest that PCL is a suitable material for studying reactive astrogliosis on electrospun nano/microfibers.

3.2.2 Culture Surfaces preparation

Random PLLA nano/microfibers are prepared using the same method as mentioned in Chapter 2.

Random PCL nano/microfibers are also prepared using the method of electrospinning. However, the parameter setup is slightly different from electrospinning PLLA. After trial and error, we found the best setup: the spinning rate of the mandrel is 3000RPM, and the distance from the needle to the mandrel is 12cm. Other parameter settings remain the same as electrospinning PLLA.

Based on our experience that fiber diameter is mainly dependent on the concentration of the polymer solution, PLLA solutions of 9%, 11%, 13% and 15% (w/v), PCL solutions of 11%, 13%, 17% and 23% (w/v) were prepared and electrospinned. After electrospinning, these samples were mounted onto a stub and sputter coated with gold. Finally, the goad coated samples were examined with Scan Electron Microscopy (SEM) to obtain high-resolution images and then the quantification of fiber diameter could be done using ImageJ.

Figure 18: SEM images of electrospun PLLA fibers

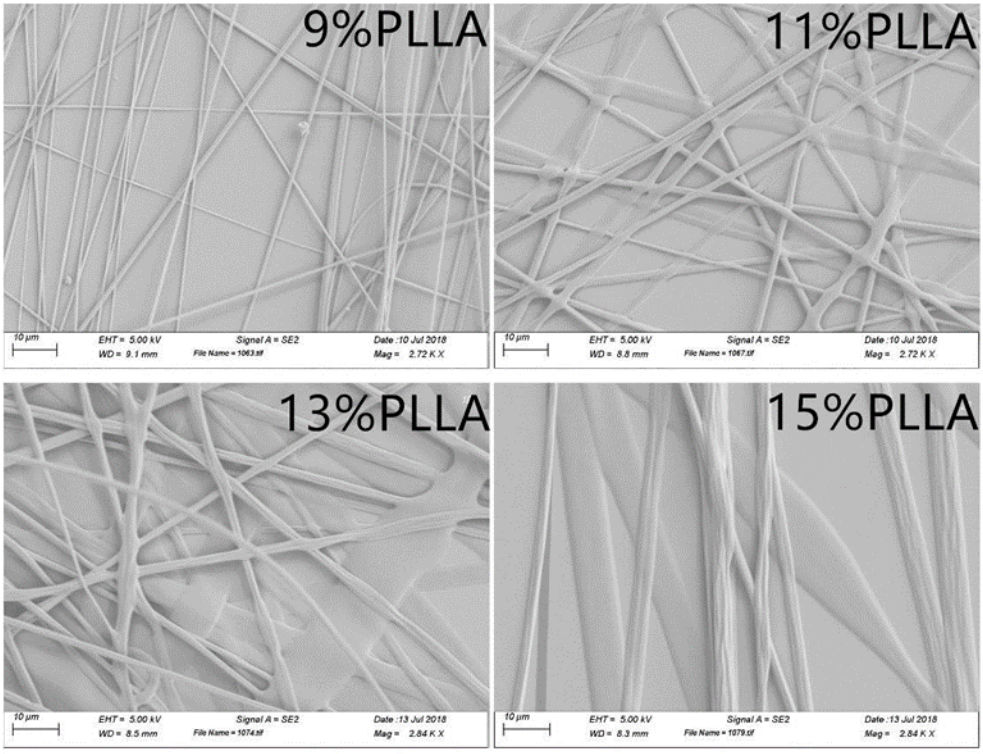

Figure 19: SEM images of PCL electrospun fibers

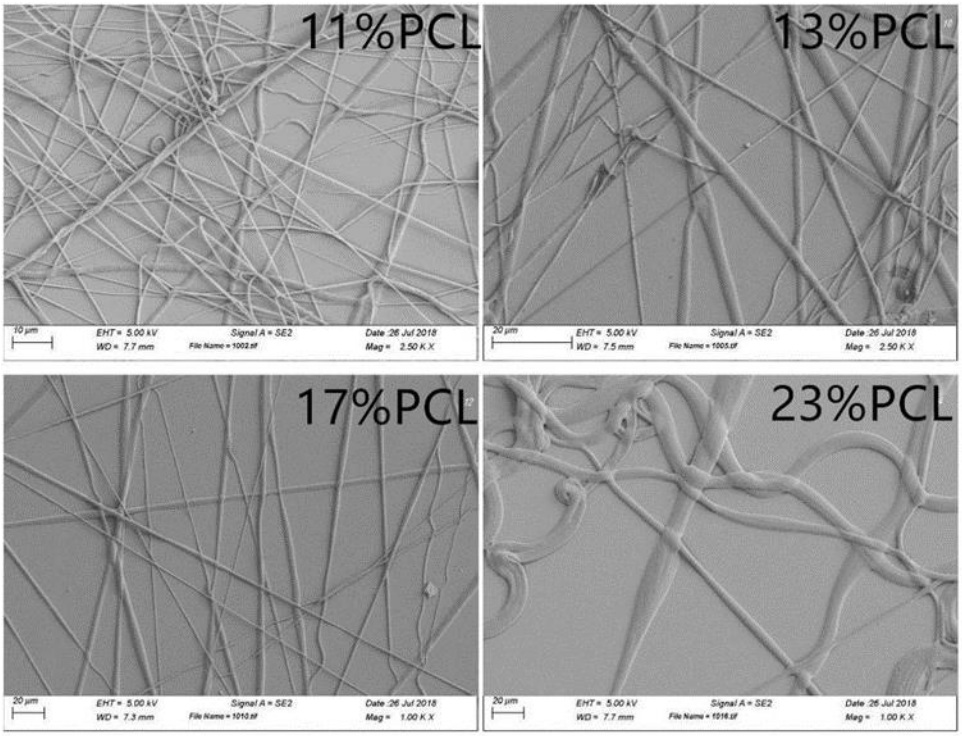

Figure 20: Fiber diameter of various electrospun scaffolds

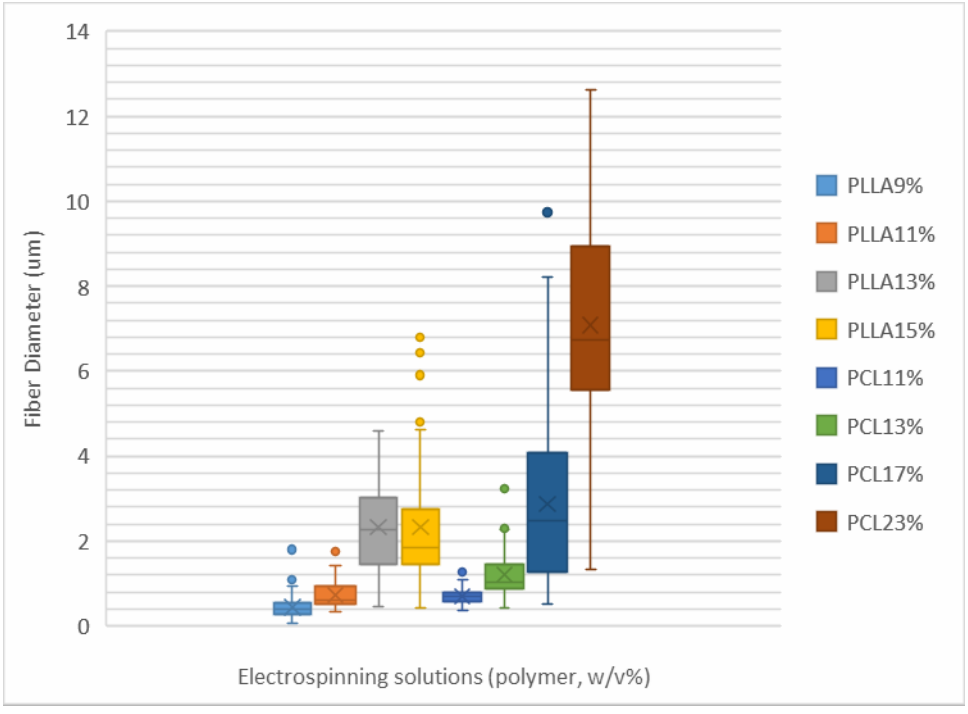

The results of the quantified fiber diameters are shown as a box and whisker plot above.

The crossings are the mean of each group. The width of the bars shows the distribution of the diameters, the thinner the bar, the narrower distribution of the fiber sizes, the better control we can gain of the fiber diameter. Outliers are automatically selected out by Excel. It seems from this plot that fibers made from 11% PLLA, 11% PCL have diameters of the same range around 1 micron, 13% PLLA, 15% PLLA and 17% PCL have diameters of the same range around 2 microns while some 17% PLLA fibers can have diameter of 3 or 4 microns. However, the gridlines here are too narrow and packed to provide more detailed information. If we pick these out and make individual plots for them, we can have smaller gridlines and wider distance in between.

Figure 21: Diameter distribution of 11% PLLA and 11% PCL

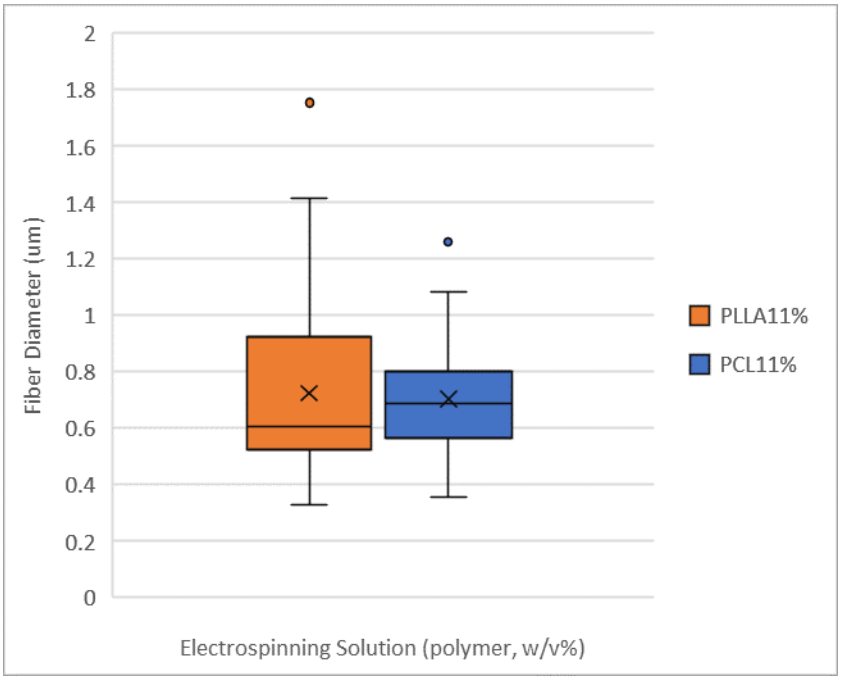

Figure 22: Diameter distribution of 13% PLLA, 15% PLLA and 17% PCL

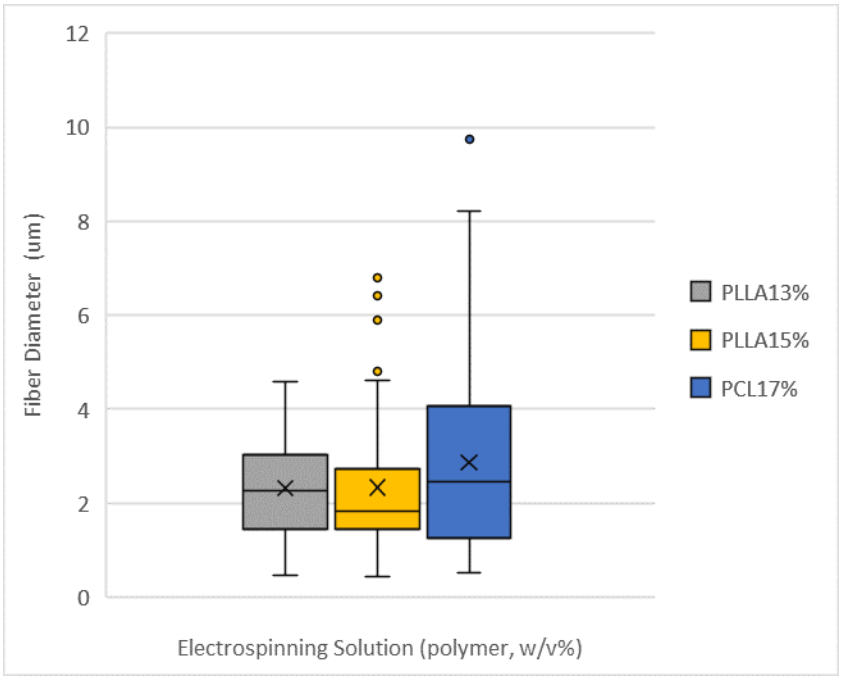

From the figure 22, it is not hard to find that the average diameter of the fibers made from 11% PLLA and 11% PCL is around 600 nanometers. We will refer to the fibers made from

11% PLLA and 11% PCL as nanofibers.

In the figure 23, all three solutions seem to achieve an average fiber diameter of around 2 microns while a quarter of fibers made from 17% PCL solutions can extend to 4 to 8 microns. We will refer to these as microfibers.

Based on the result, we can say that we had successfully achieved the goal of building scaffolds of the same fiber diameter with different materials. Fibers made from 11% PLLA, 11% PCL, 13% PLLA, 15% PLLA and 17% PCL solutions were decided to be used for the experiments.

3.2.3 Cell culture, seeding, staining and imaging

Quiescent and dbcAMP treated astrocyte culture were done following the same protocol in Chapter 2. So were the seeding, immunostaining, and imaging.

3.3 Result

3.3.1 Descriptive analysis

Figure 23: Quiescent astrocytes on nanofibers

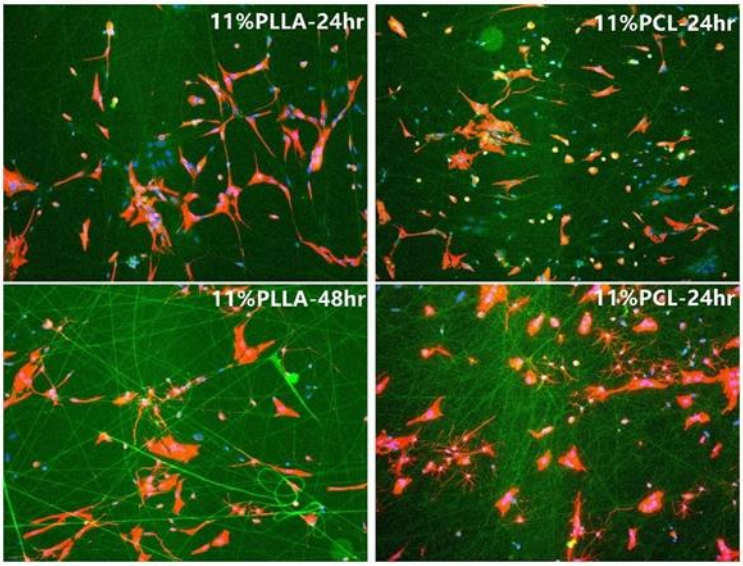

Figure 24: dbcAMP treated astrocytes on nanofibers

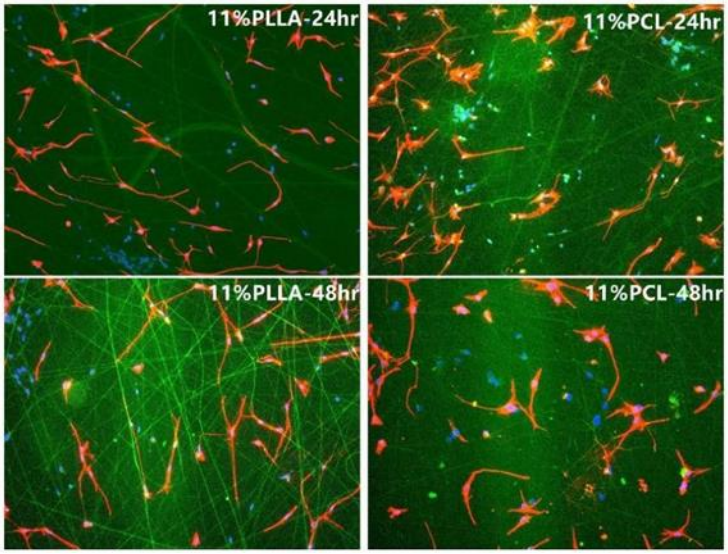

Figure 25: Quiescent astrocytes on microfibers

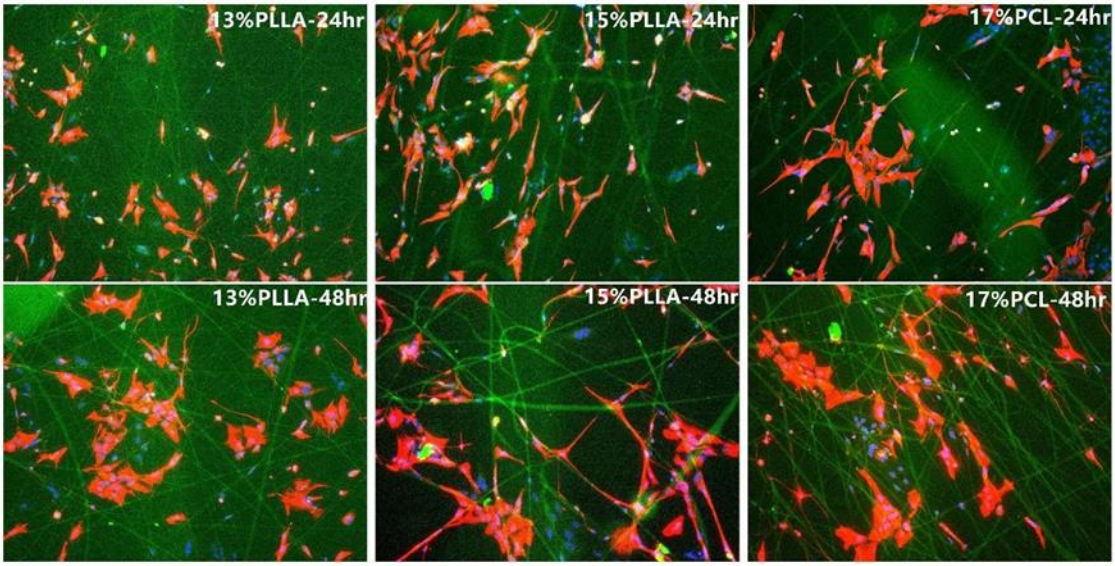

Figure 26: dbcAMP treated astrocytes on microfibers

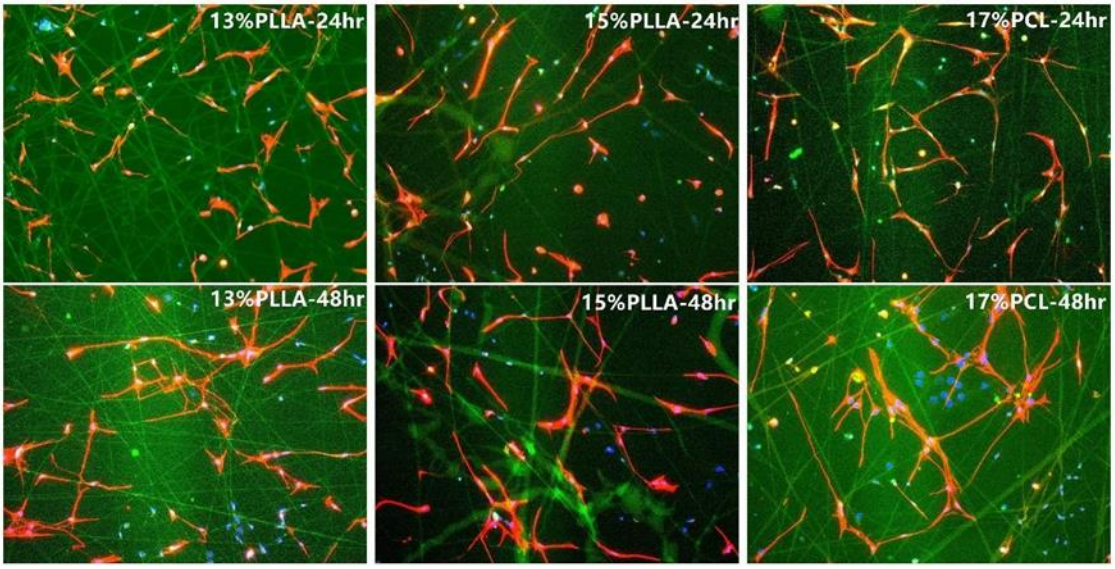

From the images it can be observed that: 1) both dbcAMP treated and quiescent astrocytes gained longer processes when they are cultured for a longer time, 2) dbcAMP treated astrocytes showed a pronounced growth in cell processes than quiescent astrocytes, 3) quiescent astrocytes tend to grow in clusters than dbcAMP treated ones, 4) the stages of

reactive astrogliosis within nanofiber or microfiber groups are identical.

3.3.2 Quantitative analysis

The part of quantitative analysis includes cell count, average single cell area, and average cell process length. Cell count can indicate whether the proliferation rates are different. Single cell area and the length of the cell can tell the extent of astrocyte hypertrophy.

Each condition has 4 coverslip samples, and for each sample two images were taken at random locations on the coverslips. These images were used for quantitative analysis. The comparisons were done within two groups: nanofibers (11% PLLA, 11% PCL) and microfibers (13% PLLA, 15% PLLA and 17% PCL). Results are discussed below.

a) Proliferation

Numbers of astrocytes per image per counted, excluding cells that are not GFAP positive. Results are plotted separately for nanofibers and microfibers.

Figure 27: Number of astrocytes on nanofibers

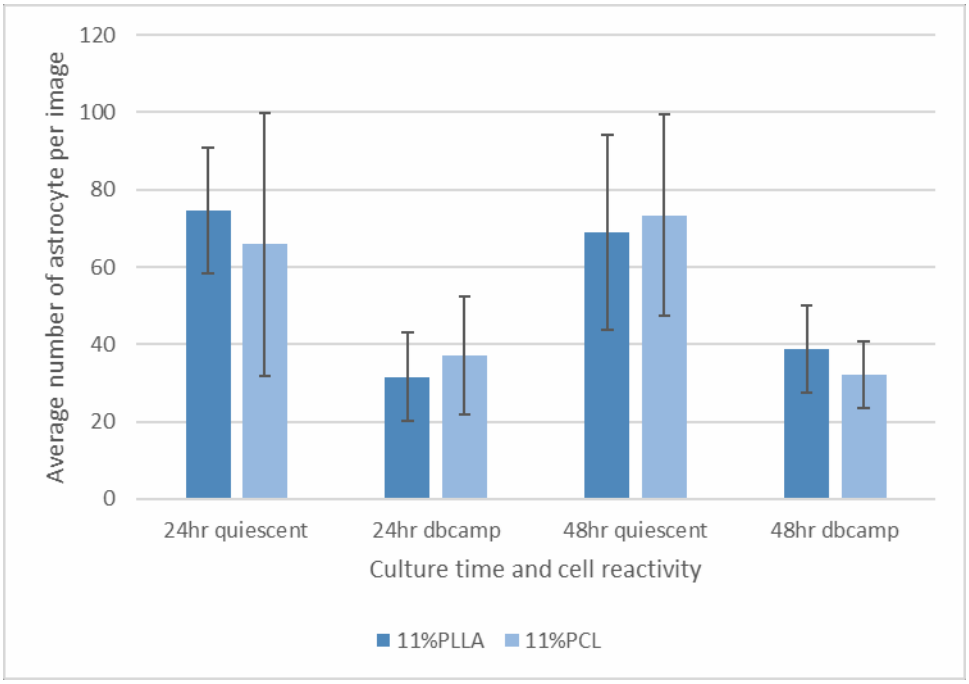

Figure 28: Number of astrocytes on microfibers

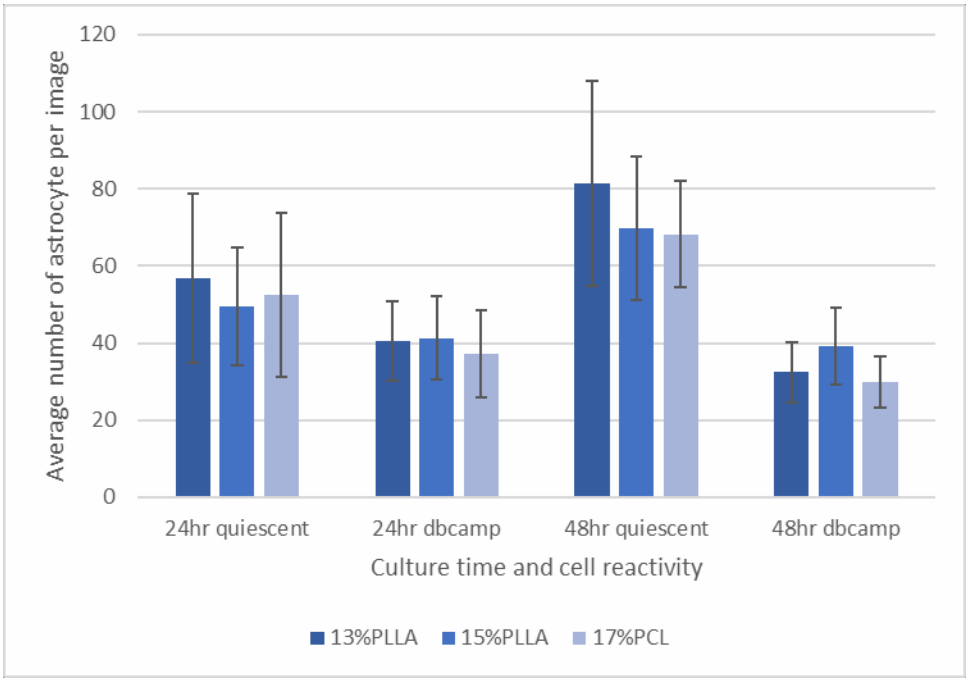

It can be observed from the plot that: 1) in same cell type and culture time scenario, the numbers of astrocytes on different fiber scaffolds that are of the same size fall in same

range, 2) numbers of astrocytes in the dbcAMP treated astrocyte seeded scaffolds are less than those in quiescent astrocyte seeded scaffolds. The first observation proved that level of cell proliferation is not related to the type of polymer. The second observation gives rise to the assumption that in the reactive astrogliosis induced by dbcAMP there might be suppressed proliferation. One-way ANOVA was done to compare the difference in nanofibers and microfibers, the P-value of 0.72 is greater than α of 0.05, which indicates that there is no difference in astrocyte proliferation on fibers of different sizes.

b) Cell Area

Single cell area can represent the extent of astrocyte hypertrophy. However, the analysis of single cells is hard to achieve because of the difficulty to measure single cell area in some clusters of astrocytes and the different morphology of some single astrocytes and astrocytes in clusters. Hence, the method developed here is to analyze the integrated density (which is the overall area of all astrocytes) of the single images and then divide averaged integrated density with corresponding average cell count. In this way, the average single cell area can be achieved without measuring cell by cell.

Figure 29: Average area of astrocyte on nanofibers

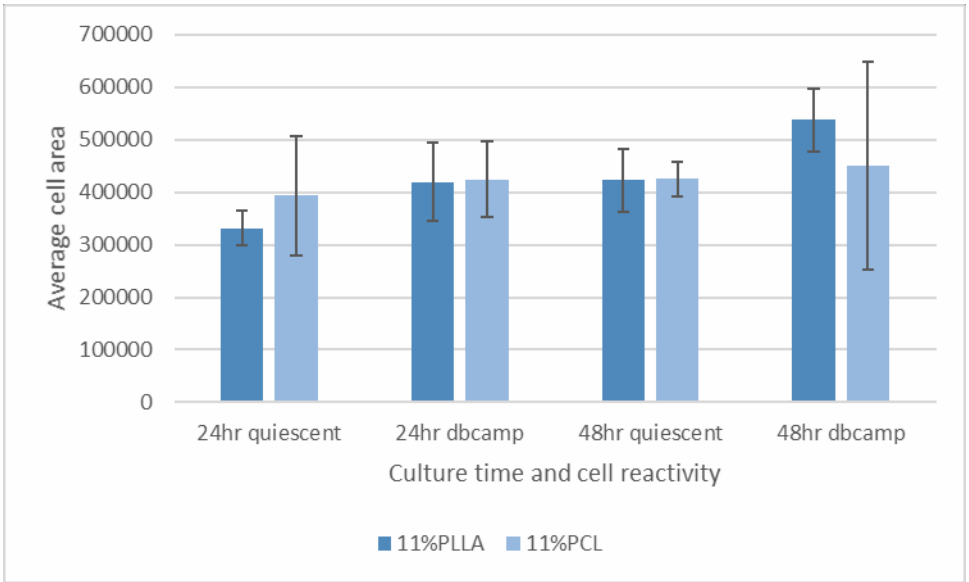

Figure 30: Average area of astrocyte on microfibers

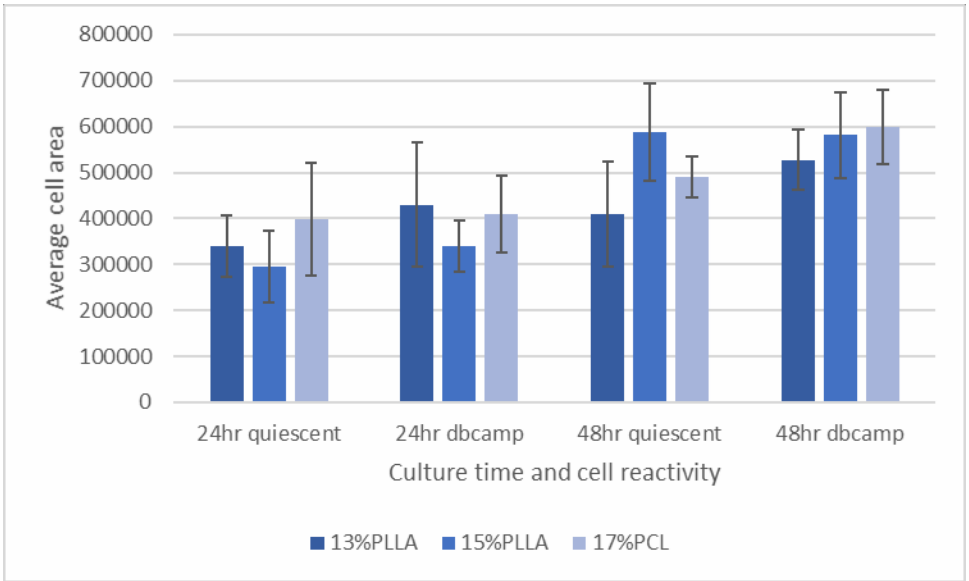

From these charts and ANOVA results, we can find: 1) astrocytes growing on nanofibers in most scenarios have average cell area of 400000 pixels, while some can grow up to 500000 pixels, 2) astrocytes seeded on microfibers after 24hr culture have an average cell area around 300000-400000 pixels, and after 48hr culture this can reach up to 600000

pixels 3) both quiescent and dbcAMP treated astrocytes cultured on nano and micro PCL fibers for 48 hours have relatively larger area than cultured for 24 hours, 4) size of the fibers do not exhibit difference in the hypertrophy of astrocytes (P=0.54>α).

c) Average Process Length

Processes' lengths of random astrocytes are measured and the averages are calculated.

Figure 31: Average process length on nanofibers

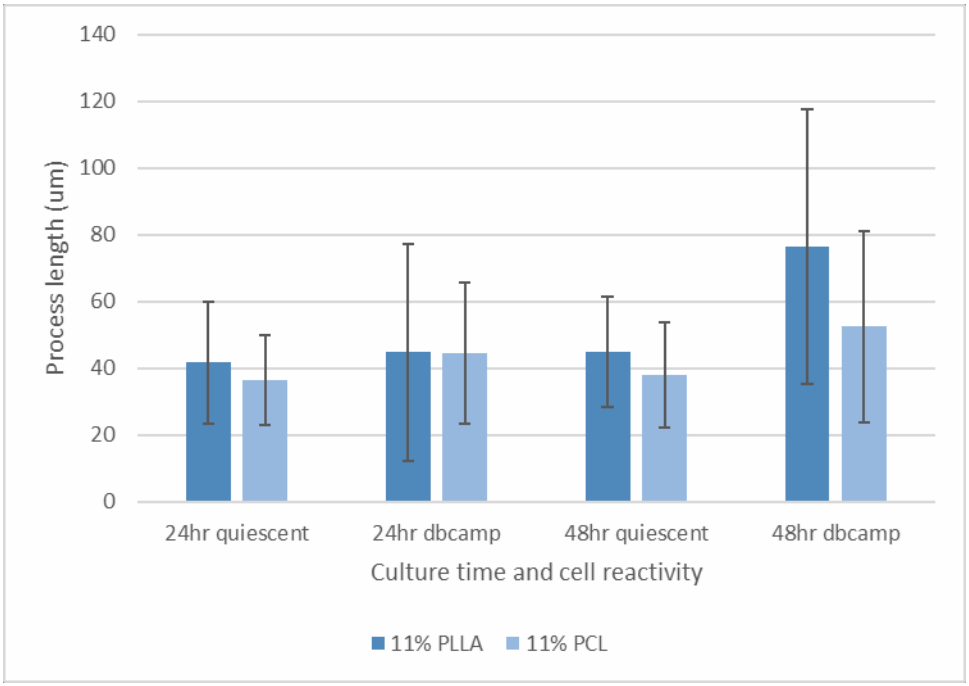

Figure 32: Average process length on microfibers

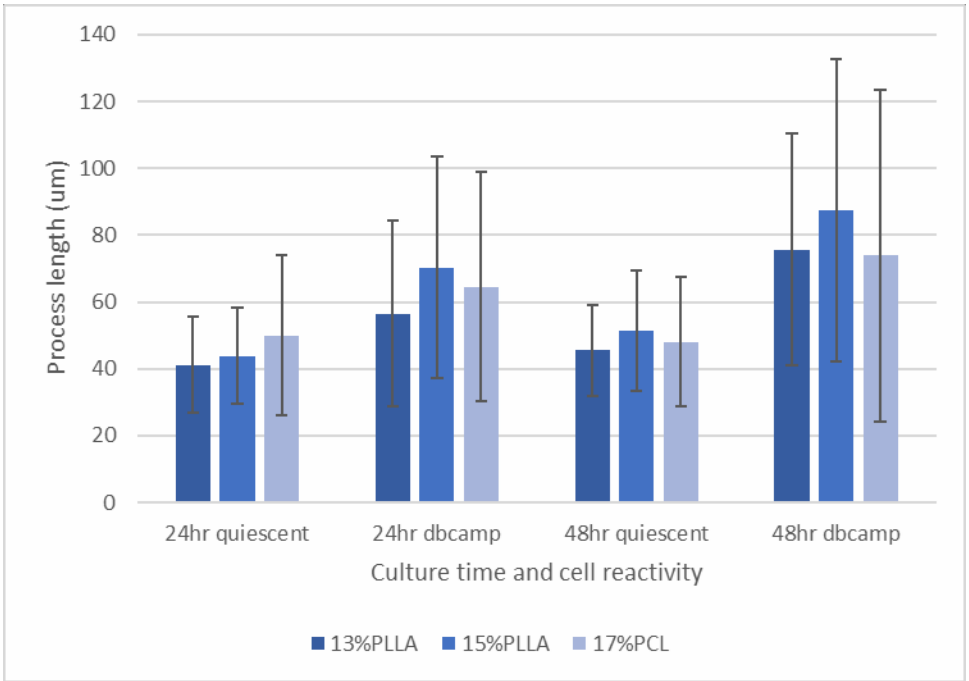

In the nanofiber plot, only dbcAMP treated astrocytes seeded scaffolds that are cultured for 48 hours have a visible increase in process length than the 3 other groups, while in the microfiber plots, dbcAMP treated astrocytes cultured for 24 and 48 hours both showed a significant increase than the quiescent groups. The error bars here represent the standard deviation, and it is found that dbcAMP treated astrocytes have a bigger standard deviation in their process length comparing to the quiescent astrocytes, which represent that dbcAMP treated astrocytes have a wider spread of their process lengths. Again, the ANOVA analysis was repeated. The P-values indicated that (1) there is no significant difference in overall astrocytes' process length on fibers of different size ($P=0.09>\alpha$), (2) there is significant difference in quiescent astrocytes' process length on fibers of different size ($P=0.03<\alpha$), (3) there is no significant difference in reactive astrocytes' process length on fibers of different

size ($P=0.07 > \alpha$), (4) there is significant difference in astrocytes' process length on cell reactivity ($P=0.0004 < \alpha$).

3.4 Conclusion

In this chapter, we have successfully achieved electrospinning PLLA and PCL fibers that have diameter in the same range: 600nm and 2 microns, and have analyzed various indicators for reactive astrogliosis. It is found with the increase of the fiber size, dbcAMP treated astrocytes tend to have significant increase in their cell area and process length.

Glial scar like clusters of astrocytes were proposed to be counted and compared, however, the resolution of our image could not provide enough detail to recognize if some astrocytes are overlapping or just growing close to each other.

The results indicate that PCL fibers induce similar reactive astrogliosis as PLLA fibers do. Also, the comparison between PLLA and PCL fibers that have the same diameter showed there is little influence of the two polymers on reactive astrogliosis.

Chapter 4 Discussion and conclusion

Let's recall the morphology change in different stages of reactive astrogliosis: in healthy CNS tissues, astrocytes have an even distribution and possess individual territories; in mild to moderated reactive astrogliosis, hypertrophy of the cell body and cell processes can be observed while individual cell domains are remained; in severe diffuse reactive astrogliosis, there are marked hypertrophy of the cell body and cell processes with disruption to individual cell domains, the boundaries of previous individual cell domains are blurred; in severe reactive astrogliosis with compact scar formation, substantial proliferation of astrocytes can be observed with hypertrophy of cell body and processes, individual cell domains are obliterated, and astrocyte scars are formed along like borders. [1,8,9]

If we summarize all the data, classify the stage of reactive astrogliosis of the astrocytes we cultured on different scaffolds and label them with different colors:

Table 1: Stages of reactive astrogliosis on random and aligned PLLA fibers

Culture Scaffold	Seeding Astrocytes	Culture Time	Stage of Reactive Astrogliosis
11% PLLA - Random	Quiescent	24 hr	Normal to mild
		48 hr	Normal to mild
	Reactive	24 hr	Moderate
		48 hr	Moderate
11% PLLA - Aligned	Quiescent	24 hr	Normal to mild
		48 hr	Normal to mild
	Reactive	24 hr	Moderate
		48 hr	Normal to moderate
13% PLLA - Random	Quiescent	24 hr	Normal to mild
		48 hr	Normal to mild
	Reactive	24 hr	Moderate
		48 hr	Moderate
13% PLLA - Aligned	Quiescent	24 hr	Moderate
		48 hr	Normal to mild
	Reactive	24 hr	Moderate to Severe
		48 hr	Moderate
15% PLLA - Random	Quiescent	24 hr	Mild to moderate
		48 hr	Moderate to severe
	Reactive	24 hr	Modertate to severe
		48 hr	**Severe with scar**
15% PLLA - Aligned	Quiescent	24 hr	Moderate
		48 hr	Moderate
	Reactive	24 hr	Mild to severe
		48 hr	**Severe with scar**

Table 2: Stages of reactive astrogliosis on PLLA and PCL electrospun nanofibers and microfibers

Culture Scaffold		Seeding Astrocytes	Culture Time	Stage of Reactive Astrogliosis
600nm-nanofiber	11% PLLA	Quiescent	24hr	Moderate
			48hr	Moderate
		Reactive	24hr	Moderate to severe
			48hr	Moderate to severe
	11% PCL	Quiescent	24hr	Moderate
			48hr	Moderate
		Reactive	24hr	Moderate to severe
			48hr	Moderate to severe
2000nm-microfiber	13% PLLA	Quiescent	24hr	Moderate
			48hr	Moderate
		Reactive	24hr	Severe
			48hr	**Severe with scar**
	15% PLLA	Quiescent	24hr	Moderate to severe
			48hr	Moderate to severe
		Reactive	24hr	Severe
			48hr	**Severe with scar**
	17% PCL	Quiescent	24hr	Moderate to severe
			48hr	Moderate to severe
		Reactive	24hr	Severe
			48hr	**Severe with scar**

The two charts and our previously discussed results showed that: 1) fiber diameter is a dominant factor in the stage of reactive astrogliosis, 2) the stage of reactive astrogliosis is

not related to the orientation of the fibers, 3) the stage of reactive astrogliosis is not related to other properties of two polymers that we have used.

Additionally, it is interesting to find that the astrocytes cultured on the aligned PLLA fiber scaffolds showed a morphology of fibrous astrocytes, that the processes are long without branching, while the primary astrocytes seeded for these experiments were protoplasmic ones obtained from the cerebellum. This observation gives rise to the hypothesis that protoplasmic astrocytes and fibrous astrocytes could be the same type of cell that are responding to different environments differently, and that the type of astrocytes may be able to change under certain circumstances. To confirm this, experiment of fibrous astrocytes seeded on random and aligned fiber scaffolds needs to be done.

However, reactive astrogliosis is not only about the morphology change of astrocytes, but also the triggered molecular pathways, uptake and release of various substances, and the change in astrocyte functions. These are vital but not studied in our project yet. Also, in this one-year research work, we have tried to electrospin other polymers that can form fibers in the same diameter range and succeeded with Nylon-6 and Nylon-12. But the study of reactive astrogliosis on these nylon scaffolds have not been practiced. In the meantime, Dr. Virginia Ayres from Michigan State University, an expert in nanostructures, has been working with the Shreiber Lab for years measuring the nanostructure of the various fiber we made and quantifying the effects of those structures on reactive astrogliosis. Analysis of the samples of random PLLA fibers cultured with astrocytes is still in progress.

The study of astrocytes responding to electrospun fibers still has a long way to go. Not only

the relevance between the morphological change of the astrocytes and various properties of the scaffolds but also the sub-cellular level changes in astrocytes responding to these scaffolds should be cleared. The relevance of reactive astrogliosis and multiple diseases also addresses the importance of clarifying triggers of reactive astrogliosis and knowing how to control it. It is hoped that eventually we will be able to tailor reactive astrogliosis and involve astrocytes in therapeutic methods for patients with CNS injuries.

References

1. Sofroniew, M. V., & Vinters, H. V. (2010). Astrocytes: biology and pathology. Acta Neuropathologica, 119(1), 7–35. Doi: 10.1007/s00401-009-0619-8.
2. Chung, W., Allen, N. J., & Eroglu, C. (2015). Astrocytes Control Synapse Formation, Function, and Elimination. Cold Spring Harbor Perspectives in Biology,7(9). Doi:10.1101/cshperspect.a020370
3. Wang, D., & Bordey, A. (2008). The astrocyte odyssey. Progress in Neurobiology. Doi:10.1016/j.pneurobio.2008.09.015
4. Eng, L. F., Ghirnikar, R. S., & Lee, Y. L. (2000). Glial fibrillary acidic protein: GFAP-thirty-one years (1969–2000). [Abstract]. Neurochemical Research, 25(9- 10), 1439-1451.
5. Hol, E. M., & Pekny, M. (2015). Glial fibrillary acidic protein (GFAP) and the astrocyte intermediate filament system in diseases of the central nervous system. Current opinion in cell biology, 32, 121-130.
6. Yang, Z., & Wang, K. K. W. (2015). Glial Fibrillary acidic protein: From intermediate filament assembly and gliosis to neurobiomarker. Trends in Neurosciences, 38(6), 364–374. Doi: 10.1016/j.tins.2015.04.003
7. Eng LF, Gerstl B, Vanderhaeghen J.J. (1970) A study of proteins in old multiple sclerosis plaques. Trans Am Soc Neurochem, 1:42
8. Sofroniew, M. V. (2009). Molecular dissection of reactive astrogliosis and glial scar formation. Trends in Neurosciences, 32(12), 638–647. Doi: 10.1016/j.tins.2009.08.002
9. Wilhelmsson, U., Bushong, E. A., Price, D. L., Smarr, B. L., Phung, V., Terada, M., … Pekny, M. (2006). Redefining the concept of reactive astrocytes as cells that remain within their unique domains upon reaction to injury. Proceedings of the National Academy of Sciences of the United States of America, 103(46), 17513– 17518. Doi: 10.1073/pnas.0602841103
10. Pekny, M., Wilhelmsson, U., & Pekna, M. (2014). The dual role of astrocyte activation and reactive gliosis. Neuroscience letters, 565, 30-38. DOI: 10.1016/j.neulet.2013.12.071
11. Bhardwaj, N., & Kundu, S. C. (2010). Electrospinning: a fascinating fiber fabrication technique. Biotechnology advances, 28(3), 325-347. DOI: 10.1016/j.biotechadv.2010.01.004.
12. LF Nascimento, M., S Araujo, E., R Cordeiro, E., HP de Oliveira, A., & P de Oliveira, H. (2015). A literature investigation about electrospinning and nanofibers: historical trends, current status and future challenges. Recent patents on nanotechnology, 9(2), 76-85.
13. Olabarria, M., & Goldman, J. E. (2017). Disorders of Astrocytes: Alexander Disease as a Model. Annual Review of Pathology: Mechanisms of Disease,12(1), 131-152. Doi:10.1146/annurev-pathol-052016-100218
14. Burda, J. E., Bernstein, A. M., & Sofroniew, M. V. (2016). Astrocyte roles in traumatic brain injury. Experimental Neurology, 275(0 3), 305–315. Doi: 10.1016/j.expneurol.2015.03.020
15. Okada, S., Hara, M., Kobayakawa, K., Matsumoto, Y., & Nakashima, Y.

(2017). Astrocyte reactivity and astrogliosis after spinal cord injury. Neuroscience research. 126:39-43 Doi: 10.1016/j.neures.2017.10.004
16. Birch, A. M. (2014). The contribution of astrocytes to Alzheimer's disease. Biochem Soc Trans. 42(5):1316-20. Doi: 10.1042/BST20140171.
17. Cabezas, R., Ávila, M., Gonzalez, J., El-Bachá, R. S., Báez, E., García-Segura, L. M., … Barreto, G. E. (2014). Astrocytic modulation of blood brain barrier: perspectives on Parkinson's disease. Frontiers in Cellular Neuroscience, 8, 211. Doi: 10.3389/fncel.2014.00211
18. Yang, C., Rahimpour, S., Albert, C. H., Lonser, R. R., & Zhuang, Z. (2013). Regulation and dysregulation of astrocyte activation and implications in tumor formation. Cellular and molecular life sciences, 70(22), 4201-4211.
19. Cregg, J. M., DePaul, M. A., Filous, A. R., Lang, B. T., Tran, A., & Silver, J. (2014). Functional regeneration beyond the glial scar. Experimental neurology, 253, 197- 207.Doi: 10.1016/j.expneurol.2013.12.024.
20. Fawcett, J. W., & Asher, R. A. (1999). The glial scar and central nervous system repair. Brain research bulletin, 49(6), 377-391. Doi.org/10.1016/S0361-9230(99)00072-6
21. Sun, D., & Jakobs, T. C. (2012). Structural remodeling of astrocytes in the injured CNS. The Neuroscientist, 18(6), 567-588. Doi: 10.1177/1073858411423441.
22. Molofsky, A. V., & Deneen, B. (2015). Astrocyte development: A Guide for the Perplexed. Glia,63(8), 1320-1329. Doi:10.1002/glia.22836
23. Yang, F., Murugan, R., Wang, S., & Ramakrishna, S. (2005). Electrospinning of nano/micro scale poly (l-lactic acid) aligned fibers and their potential in neural tissue engineering. Biomaterials, 26(15), 2603-2610. Doi: 10.1016/j.biomaterials.2004.06.051.
24. Simamola, P., & Chern, W. (2006). Poly-L-lactic acid: An overview. [Abstract]. Journal of Drugs in Dermatology,5(5), 436-40.
25. Pavia, F. C., Conoscenti, G., Greco, S., Carrubba, V. L., Ghersi, G., & Brucato, V. (2018). Preparation, characterization and in vitro test of composites poly-lactic acid/hydroxyapatite scaffolds for bone tissue engineering. International Journal of Biological Macromolecules,119, 945-953. Doi:10.1016/j.ijbiomac.2018.08.007
26. Uzun, N., Martins, T. D., Teixeira, G. M., Cunha, N. L., Oliveira, R. B., Nassar, E. J., & Santos, R. A. (2015). Poly(l-lactic acid) membranes: Absence of genotoxic hazard and potential for drug delivery. Toxicology Letters,232(2), 513-518. Doi: 10.1016/j.toxlet.2014.11.032.
27. McKeen, L. W., & Massey, L. K. (2012). The effect of sterilization on plastics and elastomers. Waltham, MA: William Andrew.
28. Malikmammadov, E., Tanir, T. E., Kiziltay, A., Hasirci, V., & Hasirci, N. (2018). PCL and PCL-based materials in biomedical applications. Journal of Biomaterials Science, Polymer Edition,29(7-9), 863-893. Doi:10.1080/09205063.2017.1394711
29. Duan, H., Ye, L., Wu, X., Guan, Q., Yang, X., Han, F., . . . Wang, Z. (2014). The in vivo characterization of electrospun heparin-bonded polycaprolactone in small- diameter vascular reconstruction. Vascular,23(4), 358-365. Doi:

10.1177/1708538114550737.
30. Kim, J., Bae, W., Kim, J., Kim, J., Lee, E., Kim, H., & Kim, E. (2013). Mineralized polycaprolactone nanofibrous matrix for odontogenesis of human dental pulp cells. Journal of Biomaterials Applications,28(7), 1069-1078. Doi:10.1177/0885328213495903